ACS Macro Letters

Letter

pubs.acs.org/macroletters

Role of Polymer Graft Architecture on the Acoustic Eigenmode Formation in Densely Polymer-Tethered Colloidal Particles

Dirk Schneider,[†] Michael Schmitt,[‡] Chin Ming Hui,[§] Rebecca Sainidou,[∥] Pascal Rembert,[∥] Krzysztof Matyjaszewski,[§] Michael R. Bockstaller,*[,‡] and George Fytas*[,†,⊥]

[†]Max Planck Institute for Polymer Research, Ackermannweg 10, 55128 Mainz, Germany

[‡]Department of Materials Science and Engineering, Carnegie Mellon University, 5000 Forbes Ave., Pittsburgh, Pennsylvania 15213, United States

[§]Chemistry Department, Carnegie Mellon University, 4400 Fifth Ave., Pittsburgh, Pennsylvania 15213, United States

[∥]Laboratoire Ondes et Milieux Complexes (LOMC), UMR CNRS 6294, University of Le Havre, 75 Rue Bellot, 76058 Le Havre Cedex, France

[⊥]Department of Materials Science and FORTH-IESL P.O. Box 1527, 71110 Heraklion, Greece

Supporting Information

ABSTRACT: The concurrent evaluation of the vibration eigenfrequencies in densely polymer-tethered particle systems ("particle brushes") by Brillouin light scattering and elastodynamic theory reveals a distinctive change of acoustic eigenmode formation associated with polymer graft modification of colloidal particles. The eigenfrequencies of particle brushes reveal a characteristic red-shift compared to uniform core-shell particles that can only be rationalized by assuming imperfect boundary conditions and anisotropic elastic properties of the graft layer. The distinct characteristics of vibration modes in particle brush materials provide direct evidence for the implications of chain confinement on the nanomechanical properties of tethered chains. The results highlight a rich and hitherto unexplored parameter-space for controlling properties and interactions in particle−brush based systems that could spur the development of hybrid materials with novel functionalities.

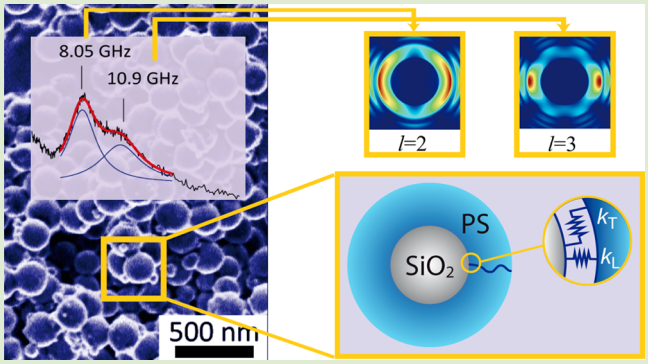

Recent progress in surface-initiated controlled radical polymerization has dramatically expanded the control over structural parameters such as grafting density, degree of polymerization, or molecular weight distribution of surface-bound chains.[1,2] The resulting ability to tailor the structural and dynamical constraints of tethered chains has fueled research on the structure-property relations of polymer-tethered particle systems and their application as hybrid materials with novel functionalities.[3−6] For densely grafted particle systems (here called "particle brushes"), the interplay between excluded volume interactions and geometrical constraints (such as particle surface curvature) gives rise to conformational transitions within the "shell" of tethered chains. The more stretched conformations of the chains in the vicinity of the particle surface sensitively affect the structure and interactions of particle brushes in solution and the solid state.[7−11] The elucidation of the role of chain conformational transitions on the physicochemical properties of brush particles therefore not only promises novel insights into the physics of microstructured colloidal systems but also holds opportunities for the design of hybrid materials with novel functionalities.

In this contribution we demonstrate that acoustic eigenmodes in brush particles distinctively differ from those of uniform spherical or core-shell particle systems.[12−15] In particular, for elastically soft or hard colloidal spheres the acoustic vibrations are localized within the particle; their eigenfrequencies depend on the materials' thermomechanical properties and are inversely proportional to the bare particle diameter.[12−15] For core-shell (silica-poly(methyl methacrylate)) particles with different polymer shell thickness but with homogeneous density, the low frequency particle resonances are mostly localized within the soft shell. The acoustic eigenvibrations in this case are well captured by elastic multipole scattering theory assuming perfect boundary conditions (PBC) that describe the propagation of elastic waves in media containing bounded objects.[14,16,17] The situation distinctly changes in the case of particle brushes, where good agreement between theoretical and experimental behavior requires the introduction of a contact stiffness (through the use of imperfect boundary conditions, IBC) to

Received: July 17, 2014
Accepted: October 3, 2014
Published: October 6, 2014

   dx.doi.org/10.1021/mz500433h | ACS Macro Lett. 2014, 3, 1059−1063

describe the coupling of the discontinuous elastic displacement field across the interface between inorganic core and polymeric shell.[18] Here, we use both (PBC and IBC) models (see Supporting Information) to evaluate the coupling of the displacement field and to estimate the corresponding contact stiffness. This contact stiffness is attributed to the stretching of densely surface-tethered chains and hence provides direct evidence for the implications of chemical confinement on the dynamical properties of brush particle systems that should be of fundamental relevance to understand (and tailor) interactions in particle-brush based materials.

The material system in our study consists of polystyrene (PS)-grafted silica particles (of radius R_0 = 57±6 nm determined by electron imaging) with systematically varied polymer graft architecture, synthesized using surface-initiated atom transfer radical polymerization (SI-ATRP).[9] The grafting density σ, degree of polymerization N(= 0−630) of the surface tethered chains and M_W/M_N of all particle brush systems are summarized in Table 1 (Sample ID: 57SiO_2-SN). Procedures for synthesis and characterization are given in the Supporting Information.

Table 1. Characteristics of Polystyrene-Tethered Silica Particle Systems[a]

Sample ID	σ (chains/nm^2)	$M_{N,GPC}$ (kg/mol)	M_W/M_N	wt % SiO_2	h_{TEM} (nm)	h_{calc} (nm)
57SiO_2-S0	–	–	–	100	–	–
57SiO_2-S130	0.61	13	1.08	81.1	7 ± 3	11
57SiO_2-S400	0.61	41	1.12	38.8	30 ± 2	26
57SiO_2-S630	0.52	65.5	1.25	23.9	44 ± 4	33

[a]The average radius of pristine silica colloids is R_0 = 57±6 nm; the layer thickness (h_{TEM}) was obtained from transmission electron microscopy (TEM) of particle monolayers, h_{calc} was determined assuming constant mass density (ρ = 1.05 g/cm^3) of the PS shell.

Figure 1a−d depicts electron micrographs of the various particle brush systems used in the present study. The interparticle distance $d = 2h$ is found to scale with the degree of polymerization of tethered chains as $d \sim N^{0.8\pm0.1}$, hence, confirming the pronounced stretching of surface-tethered chains. The stretched chain conformation can be rationalized as a consequence of excluded volume interactions in dense brushes and is consistent with predictions based on a scaling model that has been used in the past to describe chain conformational transitions in densely polymer-tethered particle systems.[8,9]

Acoustic eigenmodes of particles can be studied by BLS, Raman scattering, and time-resolved spectroscopy, depending on their dimensions.[12−15,19,20] BLS relies on the interaction between single-mode incident photons with wave vector $\mathbf{k}_i$ and thermally excited phonons along a specified direction that is determined by the scattering geometry $\mathbf{q} = \mathbf{k}_s - \mathbf{k}_i$ (with $\mathbf{k}_s$ being the wave vector of the scattered photons and $\mathbf{q}$ the scattering vector). For strongly multiple scattering systems (as in the present case), all possible values of q contribute to the observed BLS spectrum and the strongest contribution is due to $q_{bs} = 4\pi n_m/\lambda$ (n_m being the refractive index and λ the wavelength of the laser light). Hence, the number of spheroidal elastic vibrations (n, l), each characterized by the number n of vibration antinodes in the radial direction and by the angular momentum l, that can be resolved by BLS for particles of size R depends on the magnification $q_{bs}R$.[15]

Figure 2 depicts an optical image of a typical particle brush film (Figure 2a), as well as a scanning electron micrograph (Figure 2b) revealing the random microstructure of particle deposits. Only films with a thickness in the tens of micron range were evaluated to avoid substrate effects. Figure 2c−f depicts representative BLS spectra for pristine (Figure 2c) and brush particle systems (Figure 2d−f), recorded at a scattering angle of θ = 60° along with their multi-Lorentzian representation. Consistent with previous reports on the acoustic eigenspectra of (unfunctionalized) colloidal particles, the spectrum of the pristine SiO_2 particle system (Figure 2c) reveals two modes that can be attributed to the (1, 2) and (1, 3) spheroidal mode, respectively.[13,14] The peak positions reveal a systematic red-shift of eigenmodes with increasing degree of polymerization of surface grafted chains (see Figure 2d−f). The theoretical calculation of these two eigenfrequencies under assumption of perfect boundary conditions (PBC) leads to the estimation of the longitudinal c_{Ls} (= 4910 m/s) and transverse c_{Ts} (= 3090 m/s) velocity using the core radius and the mass

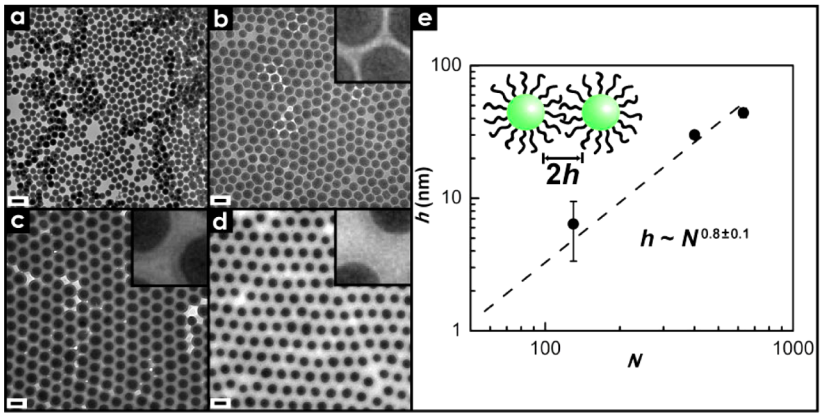

Figure 1. Characterization of 57SiO_2−SN particle brush systems. (a−d) Transmission electron micrographs of 57SiO_2−SN particle monolayers from which the brush height values h_{TEM} are obtained (Table 1): (a) N = 0 (pristine particle reference system); (b) N = 130; (c) N = 400; and (d) N = 630, respectively. Scale bar is 300 nm (a) and 200 nm (b−d). Insets show magnified image (width is 200 nm). (e) Scaling relation between h_{TEM} and N.

dx.doi.org/10.1021/mz500433h | ACS Macro Lett. 2014, 3, 1059−1063

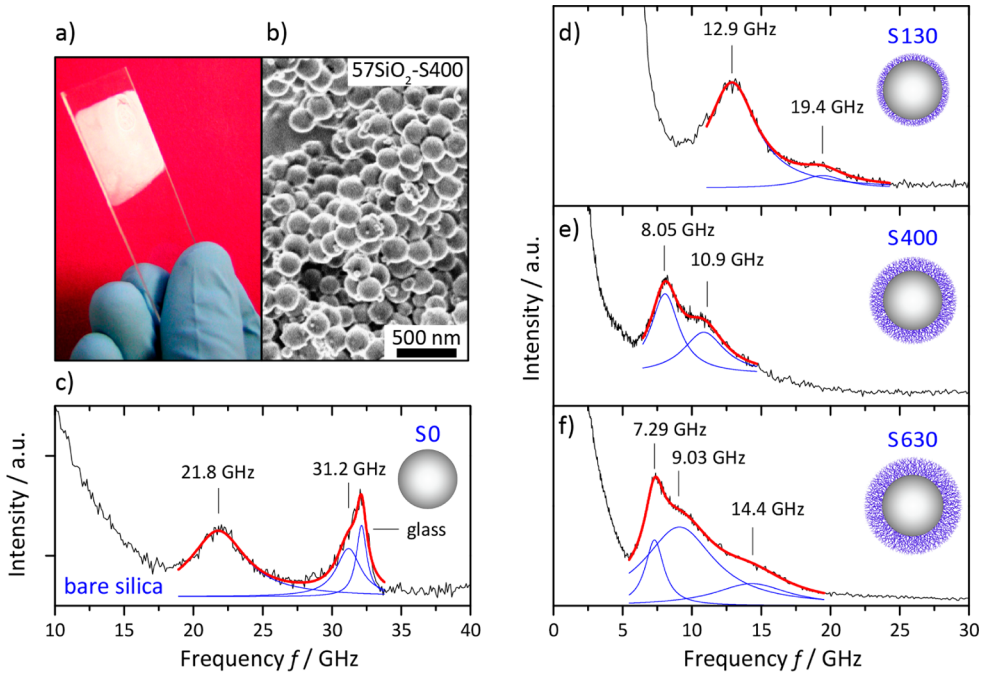

Figure 2. Photograph (a) and scanning electron micrograph (b) of disordered $57SiO_2$−S400 particle brush films used for Brillouin light scattering (BLS) analysis. (c−f) Experimental BLS vibrational spectra of random particle brush solids: (c) $N = 0$; (d) $N = 130$; (e) $N = 400$; and (f) $N = 630$. The insets illustrate the size ratio of polymer brushes and inorganic core indicated by the degree of polymerization N. The representation of the BLS spectra with up to three Lorentzians (red solid lines) to describe the individual contributions (blue) to the vibrational spectrum is shown on the Stokes side along with the values of the eigenfrequencies. In (c) note the different frequency range for the bare silica; the peak noted by "glass" indicates the longitudinal phonon of the glass substrate at a scattering angle of 60° visible due to partial transparency of the particular (thin) film.

density ρ_{SiO_2} (= 1.85 g/cm^3) as fixed parameters. In agreement with previous reports, these values are somewhat lower than those for dense amorphous glass (c_{Ls} = 5970 m/s, c_{Ts} = 3760 m/s, and ρ_{SiO_2} = 2.2 g/cm^3).[14] The Poisson's ratio $\nu = (x^2/2-1)/(x^2-1)$, where $x \equiv c_{Ls}/c_{Ts}$ assumes a similar value (0.17) as for bulk glass.

The eigenfrequencies were determined by fitting of BLS spectra with Lorentzians (solid lines) and their values are given in Figure 2c−f. With increasing brush thickness, the BLS spectrum becomes richer due to the increasing magnification $q_{bs}R$.

To reconcile the experimental eigenfrequencies of the particle brush systems, theoretical predictions for two distinct scattering configurations, corresponding to perfect (PBC) and imperfect (IBC) boundary conditions, respectively, were considered, using elastic scattering theory.[16,17] In the case of PBC, the density and the two sound velocities for the pristine silica core (obtained from Figure 2c) were assumed fixed. To further reduce the number of adjustable parameters the corresponding quantities for the PS brush were assumed equal to those of PS colloidal particles c_{LPS} (= 2350 m/s), c_{TPS} (= 1210 m/s) with ν = 0.32 and ρ_{PS} = 1.05 g/cm^3 that were determined previously.[14] The thickness h of the polymer brush was used as adjustable parameter to capture the experimental eigenfrequencies for PBC.

Figure 3a displays the theoretical prediction of the two low frequency spheroidal (*1*, *2*) and (*1*, *3*) modes based on the DOS spectra under PBC assuming a uniformly PS-coated silica (R_0 = 57 nm) as a function of the shell thickness, h, along with the experimental frequencies for all three particle brush systems.[17] To account for partial collapse of tethered chains in the case of isolated particles the thickness h_{calc} was estimated assuming a constant density of the brush layer (ρ_{PS} = 1.05 g/cm^3) resulting in a somewhat weaker scaling of $h_{calc} \sim N^{0.64}$ as compared to h_{TEM}. We note that these values also agree well with the estimated layer thickness determined from the phononic band structure of ordered films of the same particle brush systems (results not shown here); the error bar in the h values in Figure 3 reflects the spread of the different estimates.

Surprisingly, PBC calculations (see Figure 3a) systematically overestimate the experimental frequencies for all particle brush systems, even if the PS layer is modeled as a "multilayered shell" with progressively varying elastic parameters. This is in contrast to uniform silica-PMMA core-shell particles that were successfully captured by the same theory.[14] The disparity between experiment and theory under PBC is largest for N = 130 and decreases as the brush thickness increases. We note that particle size disparity cannot account for the observed trend since its main effect will be peak broadening rather than a change in peak position.[21]

The inability of the uniform core-shell model to capture the experimental eigenfrequencies is rationalized as a consequence of anisotropy across the particle-polymer interface due to the stretching of tethered chains. To account for chain stretching and anisotropy in the existing scattering model imperfect boundary conditions (IBC) were applied. The assumption of IBC implies a discontinuity in the displacement field across the silica-PS interface that is determined by $1/k_L$ and $1/k_T$, where $k_{L,T}$ correspond to the effective stiffness coefficients (spring constants) in longitudinal and transverse (i.e., normal and parallel to the interface) direction. The IBC model hence approximates the complex variation of elastic constants within the brush layer as discontinuity of the displacement field across the particle/polymer interface. Figure 3b reveals excellent agreement between the experimental data with the IBC

dx.doi.org/10.1021/mz500433h | ACS Macro Lett. 2014, 3, 1059−1063

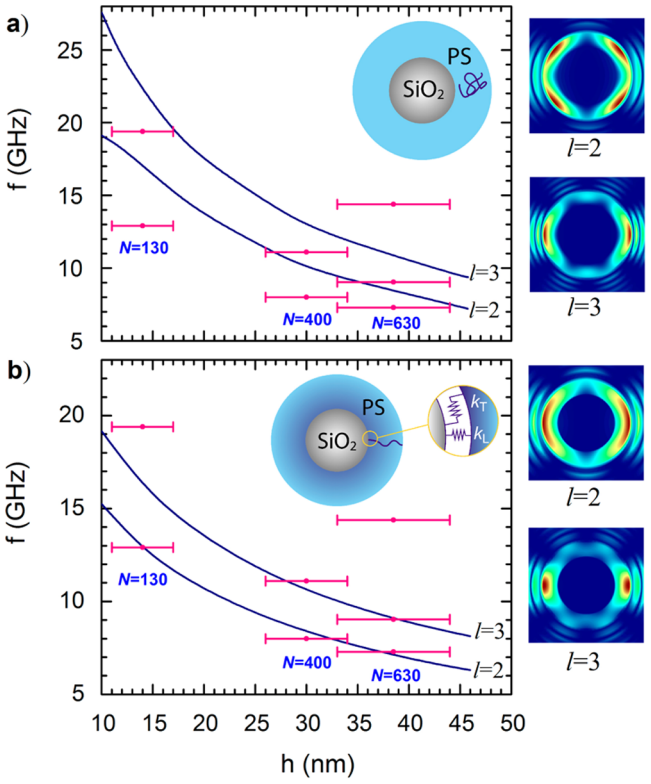

Figure 3. Calculated dispersion plots of the lowest $l = 2$ and $l = 3$ eigenfrequencies of a silica-PS core-brush particle in air as a function of the PS brush thickness, h, for (a) perfect and (b) imperfect boundary conditions applied at the interface between silica and PS. Insets depict the corresponding intensity field plots for $h = 30$ nm revealing a transition from predominantly tangential (PBC) to radial vibrating modes (IBC). The experimental values for the three samples are indicated by red dots; the horizontal red bars indicate the estimated limits for h.

predictions (where $k_L = 0.41$ GPa/nm and $k_T = 0.11$ GPa/nm have been assumed for all three particle brush systems, corresponding to spring constants in the range of 4–17 μN/nm). The agreement demonstrates that the orientation of chains (and the associated elastic anisotropy) across the particle interface profoundly alters the eigenmode formation in brush particles—a finding that bears similarity to previous reports on colloids adhered to solid surfaces.[22,23] It is interesting to note that the good fit in Figure 3b is obtained under the assumption of a unique pair of values, (k_L, k_T), for the three distinct brush systems, thus, indicating a similar "anisotropic shell" of stretched segments in all cases; this conclusion is in-line with the prediction by scaling theory that prescribes a transition from stretched to relaxed chain conformations around a "critical brush thickness" that is fixed for a given particle radius and grafting density.[8]

In conclusion, the experimental and theoretical evaluation of acoustic eigenmodes in densely tethered particle-brush systems reveals a distinctive red-shift of eigenmode resonances that can only be rationalized by assuming anisotropic impedance mismatch across the particle-polymer interface. The particle resonances thus provide, for the first time, direct experimental evidence of the anisotropic elasticity of the polymer shell that is (presumably) caused by the stretching of chains in densely tethered particle-brush systems. In a future publication we will demonstrate that these distinctive features of eigenvibrations in particle-brushes give rise to new phonon-propagation modes in particle-brush array structures that are nonexistent in uniform particle-in-polymer systems. The unique acoustic properties of particle brush materials thus highlight a rich and hitherto unexplored parameter-space for controlling properties and interactions in particle-brush based systems that could spur the development of hybrid materials with novel functionalities such as high optical and thermal conductance or coupled opto-mechanical response.

EXPERIMENTAL SECTION

Film Casting: Particle films for TEM analysis were prepared by casting from toluene solution and subsequent thermal annealing at $T = 120$ °C for 24 h. Amorphous film samples for Brillouin scattering were prepared by precipitation of particle brushes dispersed in toluene (60–65 mg/mL) in nonsolvent (water) and subsequent deposition on glass substrate.

Brillouin light scattering (BLS) was performed using a purpose-built tandem Fabry-Perot setup.[14,15] Typical accumulation time per spectrum was 60–120 min.

ASSOCIATED CONTENT

Supporting Information

Detailed information about procedures for the synthesis of particle brush materials, film preparation, and characterization, as well as simulation of phonon dispersion relations. This material is available free of charge via the Internet at http://pubs.acs.org.

AUTHOR INFORMATION

Corresponding Authors

*E-mail: bockstaller@cmu.edu.

*E-mail: fytas@mpip-mainz.mpg.de.

Notes

The authors declare no competing financial interest.

ACKNOWLEDGMENTS

This work was primarily supported by the Air Force Office of Scientific Research (via Grant FA9550-09-1-0169) and the National Science Foundation (via Grants CMMI-1234263 and DMR-0969301). M.S. acknowledges Bertucci Graduate Fellowship support. D.S. and G.F. thank Max-Planck Society and ARISTEIA Program 285 (EU, GSRT-Greece) for partial financial support.

REFERENCES

(1) Barbey, R.; Lavanant, L.; Paripovic, D.; Schuewer, N.; Sugnaux, C.; Tugulu, S.; Klok, H.-A. *Chem. Rev.* **2009**, *109*, 5437–5527.

(2) Tsujii, Y.; Ohno, K.; Yamamoto, S.; Goto, A.; Fukuda, T. *Adv. Polym. Sci.* **2006**, *197*, 1–45.

(3) Hui, C. M.; Pietrasik, J.; Schmitt, M.; Mahoney, C.; Choi, J.; Bockstaller, M. R.; Matyjaszewski, K. *Chem. Mater.* **2014**, *26*, 745–762.

(4) Fernandes, N. J.; Koerner, H.; Giannelis, E. P.; Vaia, R. A. *MRS Commun.* **2013**, *3*, 13–29.

(5) Vlassopoulos, D.; Fytas, G. *Adv. Polym. Sci.* **2010**, *236*, 1–54.

(6) Choi, J.; Dong, H.; Matyjaszewski, K.; Bockstaller, M. R. *J. Am. Chem. Soc.* **2010**, *132*, 12537–12539.

(7) Ohno, K.; Morinaga, T.; Takeno, S.; Tsujii, Y.; Fukuda, T. *Macromolecules* **2007**, *40*, 9143–9150.

(8) Dukes, D.; Li, Y.; Lewis, S.; Benicewicz, B.; Schadler, L.; Kumar, S. K. *Macromolecules* **2010**, *43*, 1564–1570.

(9) Choi, J.; Hui, C. M.; Pietrasik, J.; Dong, H.; Matyjaszewski, K.; Bockstaller, M. R. *Soft Matter* **2012**, *8*, 4072–4082.

(10) Hore, M. J. A.; Ford, J.; Ohno, K.; Composto, R. J.; Hammouda, B. *Macromolecules* **2013**, *46*, 9341–9348.

(11) Choi, J.; Hui, C. M.; Schmitt, M.; Pietrasik, J.; Margel, S.; Matyjaszewski, K.; Bockstaller, M. R. *Langmuir* **2013**, *29*, 6452−6459.
(12) Penciu, R.; Fytas, G.; Economou, E. N.; Steffen, W.; Yannopoulos, S. N. *Phys. Rev. Lett.* **2000**, *85*, 4622−4625.
(13) Kuok, M. H.; Lim, H. S.; Ng, S. C.; Liu, N. N.; Wang, Z. K. *Phys. Rev. Lett.* **2003**, *90*, 255502.
(14) Still, T.; Sainidou, R.; Retsch, M.; Jonas, U.; Spahn, P.; Hellmann, G. P.; Fytas, G. *Nano Lett.* **2008**, *8*, 3194.
(15) Still, T.; Mattarelli, M.; Kiefer, M.; Fytas, G.; Montagna, M. *J. Phys. Chem. Lett.* **2010**, *1*, 2440−2444.
(16) Brill, D.; Gaunaurd, G. *J. Acoust. Soc. Am.* **1987**, *81*, 1−21.
(17) Sainidou, R.; Stefanou, N.; Modinos, A. *Phys. Rev. B* **2004**, *69*, 064301.
(18) Huang, W.; Rokhlin, S. I.; Wang, Y. J. *J. Acoust. Soc. Am.* **1997**, *101*, 2031−2042.
(19) Portales, H.; Gouget, N.; Saviot, L.; Yang, P.; Sirotkin, S.; Duval, E.; Mermet, A.; Pileni, M. P. *ACS Nano* **2010**, *4*, 3489−3497.
(20) Petrova, H.; Lin, C.-H.; Liejer, S.de.; Hu, M.; Mclellan, J. M.; Siekkinen, A. R.; Wiley, B. J.; Marque, M.; Xia, Y.; Sader, J. E.; Hartland, G. V. *J. Chem. Phys.* **2007**, *126*, 094709.
(21) Cheng, W.; Wang, J. J.; Jonas, U.; Steffen, W.; Fytas, G.; Penciu, R. S.; Economou, E. N. *J. Chem. Phys.* **2005**, *123*, 121104.
(22) Mattarelli, M.; Montagna, M.; Still, T.; Schneider, D.; Fytas, G. *Soft Matter* **2012**, *8*, 4235−4243.
(23) Boechler, N.; Eliason, J. K.; Kumar, A.; Nelson, K. A.; Fank, N. *Phys. Rev. Lett.* **2013**, *111*, 036103.